Pull-out strength of perforated steel plates with oval-shaped perforation

Fujinaga, Takashi

Tanaka, Teruhisa

(Citation)
Japan Architectural Review,6(1):e12363

(Issue Date)
2023-01

(Resource Type)
journal article

(Version)
Version of Record

Japan Architectural Review
Open Access
Architectural Institute of Japan

Original Paper

Pull-out strength of perforated steel plates with oval-shaped perforation

Takashi Fujinaga[1] and **Teruhisa Tanaka**[2]

[1]Research Center for Urban Safety and Security, Kobe University, Kobe, Japan [2]Department of Architecture, Faculty of Engineering, Fukuoka University, Fukuoka, Japan

Correspondence
Takashi Fujinaga, Research Center for Urban Safety and Security, Kobe University, Kobe, Hyogo 657-8501, Japan.
Email: ftaka@kobe-u.ac.jp

Funding information
Japan Society for the Promotion of Science, Grant/Award Number: 20K04771; Japan Iron and Steel Federation

Received November 15, 2022; Accepted April 18, 2023

doi: 10.1002/2475-8876.12363

Abstract

The use of Perfobond Leisten (PBL) shear connectors in building structures has attracted increasing interest. A new approach for using perforated steel plates in concrete-filled steel tube (CFST) column splices was implemented in this study. The shape of the perforation opening in perforated steel plates is generally a circle, similar to that of PBL shear connectors. However, in this study, an oval-shaped perforation was used to increase the double shear area of the concrete. A pull-out experiment was conducted on perforated steel plates with oval-shaped perforations in a CFST block to evaluate the tensile performance of the perforated steel plates. A total of 29 specimens were tested, and the pull-out strengths of the perforated steel plates were determined and analyzed under passive confinement from the steel tube. The contribution of the stress transfer was discussed in terms of the double shear of the concrete in the perforation and the bond and/or friction between the surface of the steel plate and concrete. Formulas for determining the maximum pull-out strength were also developed.

Keywords
bond, double shear, friction, mechanical shear connector, perfobond shear connector

1. Introduction

In column splices of concrete-filled steel tubes (CFSTs), the steel tube parts of the upper and lower columns are commonly joined by onsite full penetration weld while ensuring the strength of both steel tubes. The strength of the splices should be maintained even if partial welding or bolt joints are used.[1] In recent years, the shortage of welding workers has become a significant concern, in addition to the difficulty in realizing full-strength joints between super-high-strength steel material.

The authors focused on the existence of filled concrete in steel tubes and proposed a CFST column splice that transmits stresses between steel tubes through the infilled concrete using the shear resistance of perforated steel plates between the steel and the concrete[2] (see Figure 1). The proposed CFST column splice can be employed to connect perforated steel plates to a steel tube using only fillet welds and it does not utilize full penetration welds that require high-quality welding skills, such as a conventional column splice. Perfobond Leisten (PBL) shear connectors are commonly used as shear connectors between the floor slabs and steel girders of bridges.[3] The use of PBL in architectural buildings has attracted increasing research interest, because of the superior structural performance of PBL compared to that of headed studs, which are commonly used shear connectors, in a small range of displacements. However, the section sizes of architectural buildings are smaller than those of civil engineering structures. Therefore, it is difficult to apply PBL to architectural buildings because it can lead to crack initiation in concrete. The proposed column splice is assumed to have a small effect on the section size and can effectively utilize the high initial slip rigidity. In addition, the shear slip resistance can be improved by the lateral confinement of the steel tube.

Furthermore, PBL is generally used as shear slip-resistance elements between steel and concrete. However, fillet-welded perforated steel plates resist via concrete as tensile elements in the proposed column splice. Therefore, the use of tensile resistance elements and their double shear resistance behaviors have not been examined extensively. In Japan, the "AIJ Recommendations for Structural Design of Steel-concrete Shear Connections[4]" was published in 2022. However, the use of shear connectors subjected to a pull-out force is unacceptable per these recommendations because of the paucity of available experimental data. The authors previously conducted an

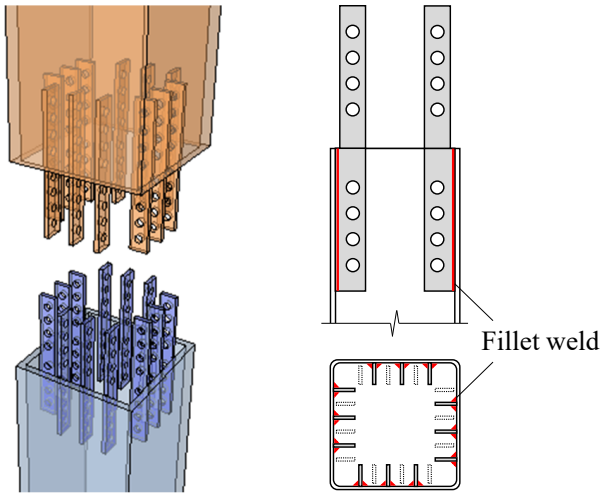

FIGURE 1. Prototype of CFST column splice using perforated steel plates[2]

experiment on perforated steel plates embedded in a CFST block subjected to tensile force under passive confinement by a steel tube, and examined the effect of the number of perforations and embedded length of perforation on the pull-out strength of perforated steel plates.[5] Additionally, besides the authors' experiments, pull-out experiments on perforated steel plates embedded in steel tubes are yet to be conducted.

In addition, the PBL perforation shape is normally a circle; however, the double shear area of the concrete can be increased by using an oval-shaped perforation. Zheng et al. conducted a parametric experiment on long-hole perfobond shear connectors parametrically to determine the shear capacity of PBL with an oval-shaped perforation.[6]

In this study, a pull-out experiment on perforated steel plates with oval-shaped perforations embedded in a CFST block was conducted to clarify the basic pull-out performance of the perforated steel plates to be attached to the CFST column splices and to determine the tensile capacity of the perforated steel plates. The shear area of the concrete in the perforation could be increased using an oval-shaped perforation, which would decrease the splicing length of the column splices. A total of 29 specimens were tested, and a calculation method for the pull-out strength of perforated steel plates with oval-shaped perforations was developed. The length of the oval-shaped perforation for the double shear of concrete that would effectively resist tensile force was discussed.

2. Pull-Out Experiment of Perforated Steel Plates with Oval-Shaped Perforation

2.1 Outline of experiment

Figure 2 and Table 1 present the dimensions of the specimens. The perforated steel plate was embedded in the center of a square CFST block (length: 290 mm, tube thickness: 6 mm) with a width and depth of 250 mm. The width of the perforated steel plate (SM490A) was 90 mm and its thickness was 22 mm ($f_y = 356$ MPa). The experimental parameters included the shape of the perforation and compressive strength of the concrete. A circular or oval-shaped perforation was formed in the embedded part by laser cutting. The diameter of the circular perforation and the edge arc of the oval-shaped perforation were both 35 mm. For the specimens with circular perforations, the number of perforations was 1 or 2. For the specimens with oval-shaped perforations, the length between the center of the edge arc was 35 mm or 70 mm. The designed compressive strength of the concrete was 21 and 45 MPa. The concrete was placed upside-down in the steel tube blocks to prevent bleeding at the upper part of the perforation, as shown in Figure 2. The top of the steel tube and concrete are flush at the top end. A form release agent to the surfaces of the steel plates of all specimens to remove the bond between the steel plate and concrete. Additionally, a styrene board of 1 mm was attached to the side of the steel plate to remove the bond between the steel and concrete almost completely. The 1 mm styrene board considerably decreased the bond/friction strength between the steel and concrete.[7] The perforated plate specimens were designed to ensure double shearing of the concrete inside the perforation prior to the other parts.

Figure 3 illustrates the loading apparatus used in this study. Pull-out concentric monotonic loading was applied using a hydraulic jack. The CFST block was fixed using PC tendons and fixing beams. The fixing beams fasten the top surface of the steel tube and concrete to prevent slipping between the steel tube and concrete and the pull-out failure of concrete. The relative displacement of the steel plate and concrete was measured using displacement transducers. Figure 4 shows the positions of the displacement transducers, and Figure 5 depicts the positions of the strain gauges on the surface of the perforated steel plate. Four gauges were placed 35 mm above and below the center of the edge arc of the perforation. Two gauges were placed on the sides of the perforation.

2.2 Relationship between bond and/or friction stress and relative displacement

Figure 6 shows the bond and/or friction stress f_{bf} versus the relative displacement relationship of the specimens with no perforation (21-0 series, 45-0 series). The blue lines indicate the behavior of the 21-0 series specimens, and the red lines represent that of the 45-0 series specimens. The bond and/or friction stress f_{bf} was obtained by dividing the measured pull-out force at the steel plate surface area on the long side of section A_b. The steel plate surface area on the long side of section A_b was derived by reducing the area of the perforation from the area obtained by multiplying the plate width by the embedded length. For specimens with no perforation, the relative slip displacement at the maximum pull-out strength was very small, and the tensile strength decreased drastically after the maximum strength was achieved. The maximum bond and/or friction stress $f_{bf,\ \max}$ was 0.542 and 1.061 MPa for the 21-0 series and 45-0 series specimens, respectively. The average bond and/or friction stress at a relative displacement of 2 mm $f_{bf,\ 2\,\mathrm{mm}}$ was 0.362 and 0.666 MPa for the 21-0 series and 45-0 series specimens, respectively. The effects of concrete strength on the maximum bond and/or friction stress $f_{bf,\ \max}$ and of average bond and/or friction stress on the relative displacement of 2 mm $f_{bf,\ 2\,\mathrm{mm}}$ can be observed. The relative displacement of 2 mm was selected as the displacement after which the bond and/or friction stress was stable. The measured maximum bond and/or friction stress exceeded the calculated maximum shear stress (0.350 MPa) without confinement at the grease-applied surface in Ref. [8], even for the Fc21 series. The Fc45 series specimen exhibited larger shear stress, and the residual shear stress exceeded the calculated stress reported in Ref. [8].

The bond and/or friction stress is affected by the concrete strength and expressed in an exponentiation form in this study. The exponent of the compressive strength of concrete, that is, the ratio of the bond and/or friction stress with both the

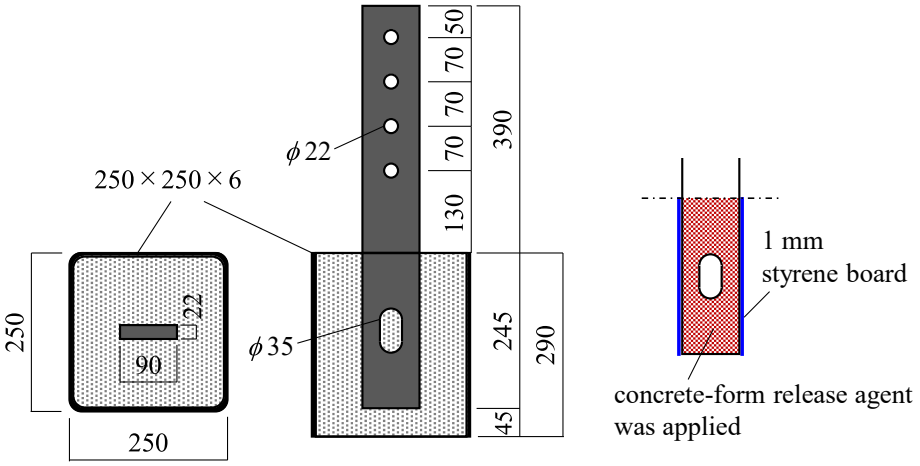

FIGURE 2. Dimensions of the specimen (unit: mm)

TABLE 1. Dimensions of the specimens

Specimens	F_c (MPa)	Number of perforations	Shape of perforation	Shape of steel plate	A_b (mm^2)	A_{ds} (mm^2)
21-0-1, 2, 3 45-0-1, 2, 3	21 45	–	–	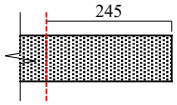	44 100	–
21-1C-1, 2, 3 45-1C-1, 2, 3	21 45	1	Circle	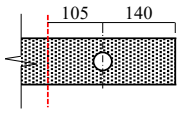	42 176	1924
21-2C-1, 2, 3 45-2C-1, 2, 3	21 45	2		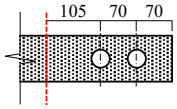	40 252	3848
21-1L35-1, 2, 3 45-1L35-1, 2, 3	21 45	1	Oval-shape 35 mm	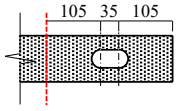	39 726	4374
21-1L70-1, 2, 3 45-1L70-1, 2	21 45		Oval-shape 70 mm	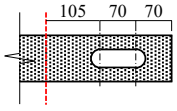	37 276	6824

Note: F_c, designed strength of concrete; A_b, surface area on the long side of the section; A_{ds}, double shear area of concrete.

maximum stress and at a relative displacement of 2 mm become small, is approximately 0.8, which can be expressed as shown in Equations (1) and (2).

$$f_{bf,\max} = 0.038 \times {f_c}^{0.8} \quad (1)$$

$$f_{bf,2\ \mathrm{mm}} = 0.025 \times {f_c}^{0.8} \quad (2)$$

where $f_{bf,\ \max}$ and $f_{bf,\ 2\ \mathrm{mm}}$ represent the maximum bond and/or friction stress and the average bond and/or friction stress on the relative displacement of 2 mm, respectively. Further, f_c represents the compressive strength of concrete (MPa).

The coefficients in Equation (1) were obtained by utilizing a trial-and-error method until the residual error from the measured behavior became small. The values obtained by applying Equations (1) and (2) are indicated by the dashed green lines and green circles in Figure 6.

2.3 Relationship between pull-out force and relative displacement

Figure 7 shows the relationship between the pull-out force and relative slip displacement of the perforated steel plate specimens. The blue lines indicate the measured behaviors of the Fc21 series specimens, whereas the red lines represent those of

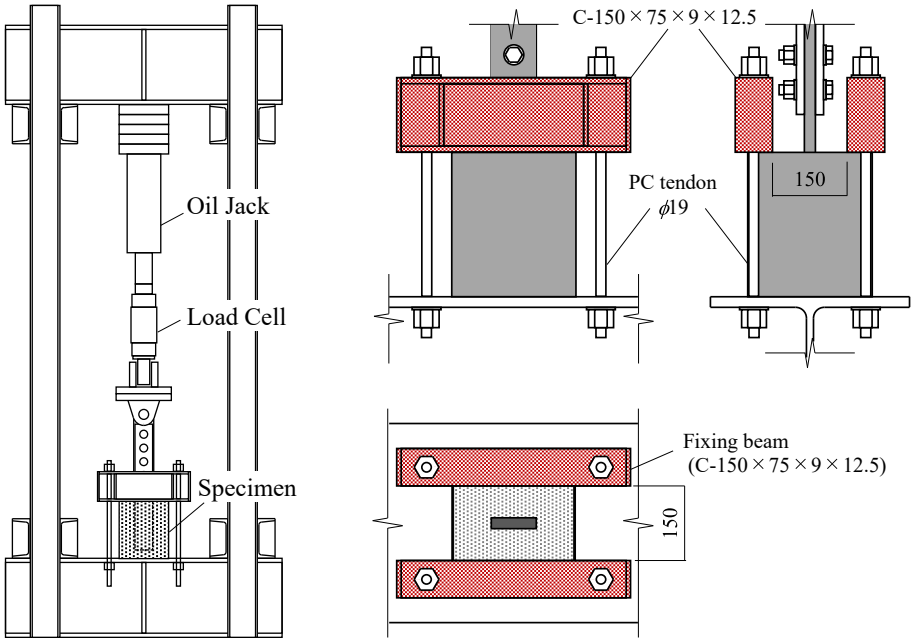

FIGURE 3. Experimental set-up

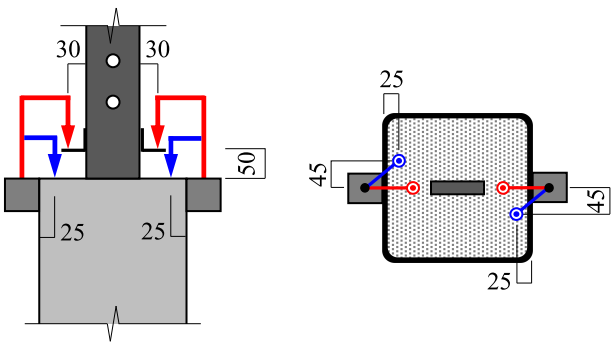

FIGURE 4. Positions of displacement transducers (unit: mm)

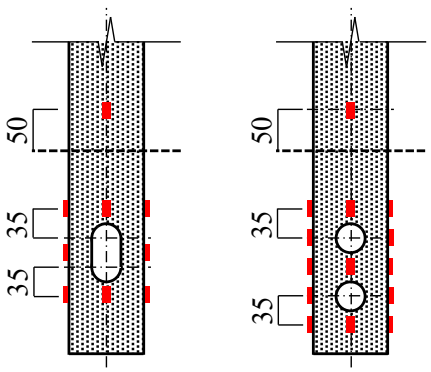

FIGURE 5. Example positions of strain gauges (unit: mm)

the Fc45 series specimens. The behaviors of the perforated steel plate specimens after the maximum pull-out strength showed that they have higher load-carrying capacities than those without perforations. The relative slip displacement at the maximum strength was larger if the shear area at perforation was large. The strength and behavior variations of the Fc45 series were larger than those of the Fc21 series. The failure mechanism was the double shear of the concrete at perforation for all specimens. The Fc45 series specimens with larger concrete strength had larger maximum strength and residual pull-out strength than those of the Fc21 series specimens; the effect of the concrete strength was observed. In the steel plates with circular perforations, the deterioration in the behavior of the Fc45 series specimens after the maximum strength was slightly steeper than that of the Fc21 series specimens, although this trend was not observed for the steel plates with oval-shaped perforations. The measured maximum pull-out strengths and the slip displacements at maximum strength are listed in Table 2.

Figure 8 depicts the relationship between the double shear strength of the concrete in the perforation and shear areas. The double shear strength at the maximum pull-out strength P_{ds} was evaluated by reducing the equivalent bond and/or friction strength from the maximum pull-out strength of each specimen using the bond and/or friction stress versus the slip displacement behavior (Section 2.2). The mean of the corresponding strengths of the three specimens with the same shape was used as the equivalent bond and/or friction strength. Figure 8 shows that the double shear strength and double shear area have an almost linear relationship for the perforated steel plates; the larger the double shear area of the concrete in the perforation, the larger the double shear strength P_{ds}. The strength per unit area P_{ds}/A_{ds} was obtained by dividing the double shear strength at the perforation P_{ds} by the double shear area of the concrete (A_{ds}). In this study, A_{ds} means twice the area of the perforation. The strengths per unit area of the Fc21 series specimens varied from approximately 30 MPa to approximately 35 MPa, and that of the Fc45 series specimens varied from approximately 40 MPa to approximately 60 MPa, although some variations can be observed. The effect of the shape of the perforation on P_{ds}/A_{ds} was not observed.

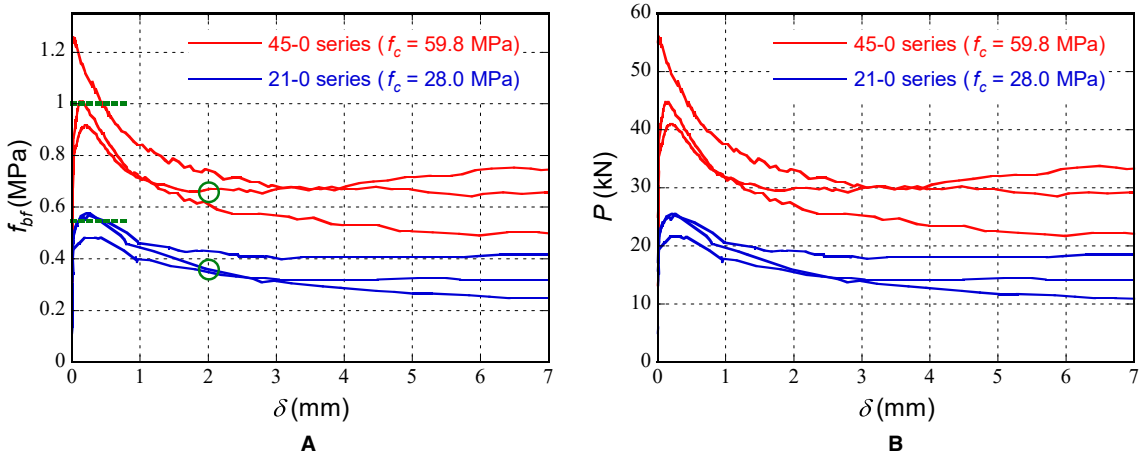

FIGURE 6. Behavior of specimens with no perforation. (A) Bond and/or friction stress versus relative pull-out displacement relationship. (B) Pull-out force versus relative pull-out displacement relationship

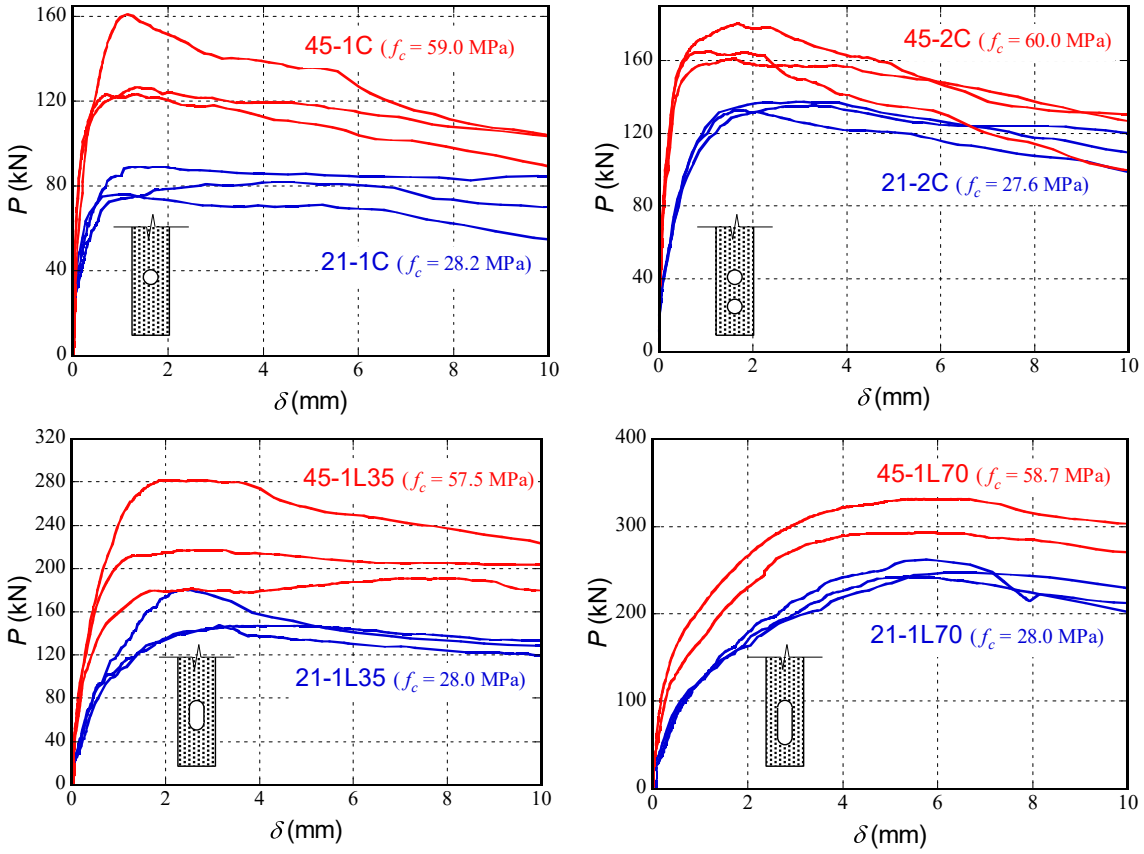

FIGURE 7. Pull-out force versus relative pull-out displacement relationship of perforated steel plate specimens

Figure 9 presents the relationship between the relative slip displacement and double shear area when the pull-out force reaches 0.9 times the maximum pull-out strength $_{exp}P_{max}$ before reaching the maximum strength. The larger the double shear area at the perforation, the larger the relative slip displacement at a strength 0.9 times the maximum pull-out strength. For the oval-shaped perforation specimens that the length between the two edge arc centers was 70 mm, the relative slip displacement at the maximum strength was larger than 2 mm. If the length of the adopted perforation is longer, the assumed design strength needs to be estimated moderately, and the strength at a small slip displacement should be ensured. Therefore, the length between the centers of both edge arcs should be the same as the perforation diameter or shorter.

Further, the relative slip displacement at the maximum strength decreased at a larger concrete strength. Although a further examination is necessary, this factor is one of the reasons why stronger concrete is more rigid and occurs during

TABLE 2. Experimental results

Shape and number of perforations	Specimens	Strength of concrete (MPa)	Max. strength $_{exp}P_{max}$ (kN)	Slip displacement at 0.9 $_{exp}P_{max}$ (mm)	Specimens	Strength of concrete (MPa)	Max. strength $_{exp}P_{max}$ (kN)	Slip displacement at 0.9 $_{exp}P_{max}$ (mm)
No perforation	21-0-1	27.7	25.3	0.240	45-0-1	59.8	56.0	0.012
	21-0-2	28.2	21.5	0.187	45-0-2		44.8	0.117
	21-0-3		25.5	0.215	45-0-3		41.0	0.187
1 Circle	21-1C-1		89.3	1.232	45-1C-1		123.5	0.684
	21-1C-2		81.8	4.195	45-1C-2		126.8	1.353
	21-1C-3		76.3	1.100	45-1C-3	57.5	161.0	1.149
2 Circle	21-2C-1	28.5	132.8	1.644	45-2C-1	60.0	161.0	1.554
	21-2C-2	27.2	137.5	3.077	45-2C-2		180.0	1.665
	21-2C-3		135.3	3.252	45-2C-3		165.0	1.091
1 Oval 35 mm	21-1L35-1	28.5	147.5	3.147	45-1L35-1	57.5	217.3	2.988
	21-1L35-2		180.5	2.407	45-1L35-2		281.5	1.960
	21-1L35-3	27.2	147.3	4.304	45-1L35-3		190.8	6.979
Oval 70 mm	21-1L70-1	28.5	242.3	5.299	45-1L70-1		292.5	5.633
	21-1L70-2		261.8	5.759	45-1L70-2	60.0	331.5	6.480
	21-1L70-3	27.2	247.0	6.124				

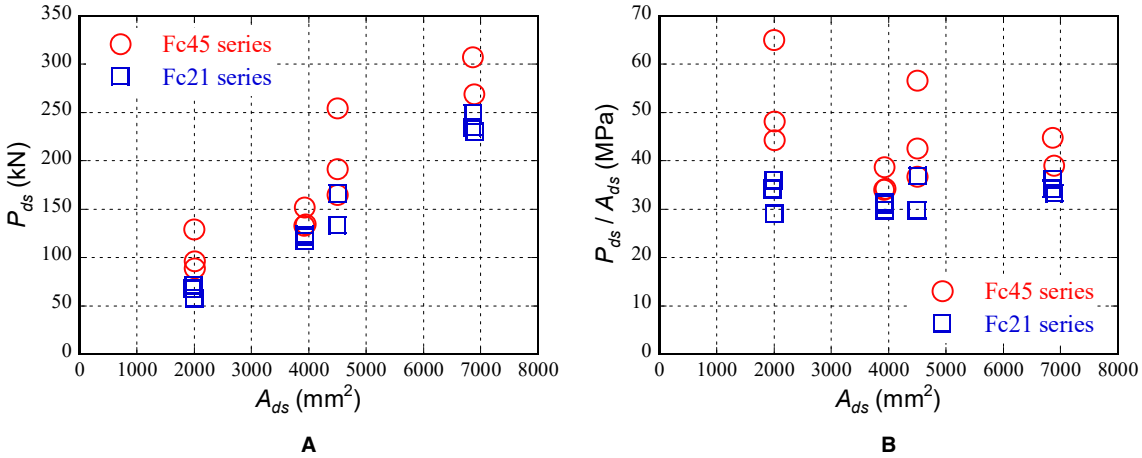

FIGURE 8. Double shear strength versus shear area relationship. (A) Double shear strength at the perforation. (B) Double shear strength per unit area

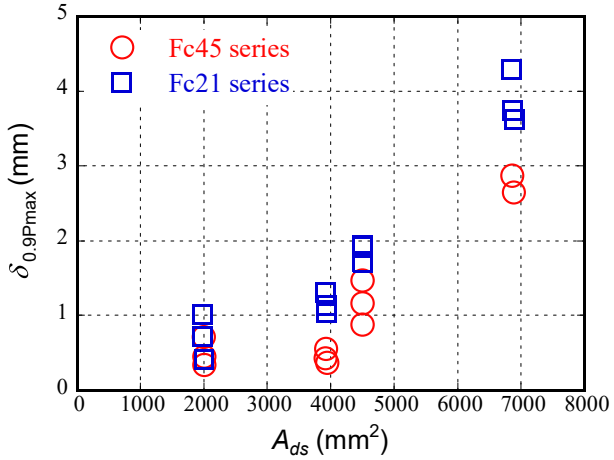

FIGURE 9. Relative slip displacement versus shear area relationship

double shear resistance in the perforation. The steel plates with oval-shaped perforations can be used in CFST column splices. The strength of the concrete in CFST tends to be high; therefore, it is advantageous for the relative slip displacement to be lower with an increase in concrete strength.

2.4 Load bearing ratio of double shear at the perforation and bond and/or friction

To determine the contribution of stress transfer attributed to the double shear of the concrete in the perforation and the bond and/or friction between the surface of the steel plate and concrete, the net axial resistances at several sections of the steel plate were derived using data from strain gauges placed on the steel plate. The shear resistance at perforation (P_s), bond and/or friction force above the first perforation (P_{bf}), and bond and/or friction force below the deepest perforation (P_{bfe}) were determined based on differences between the axial forces in each section. Each shear resistance and bond and/or friction

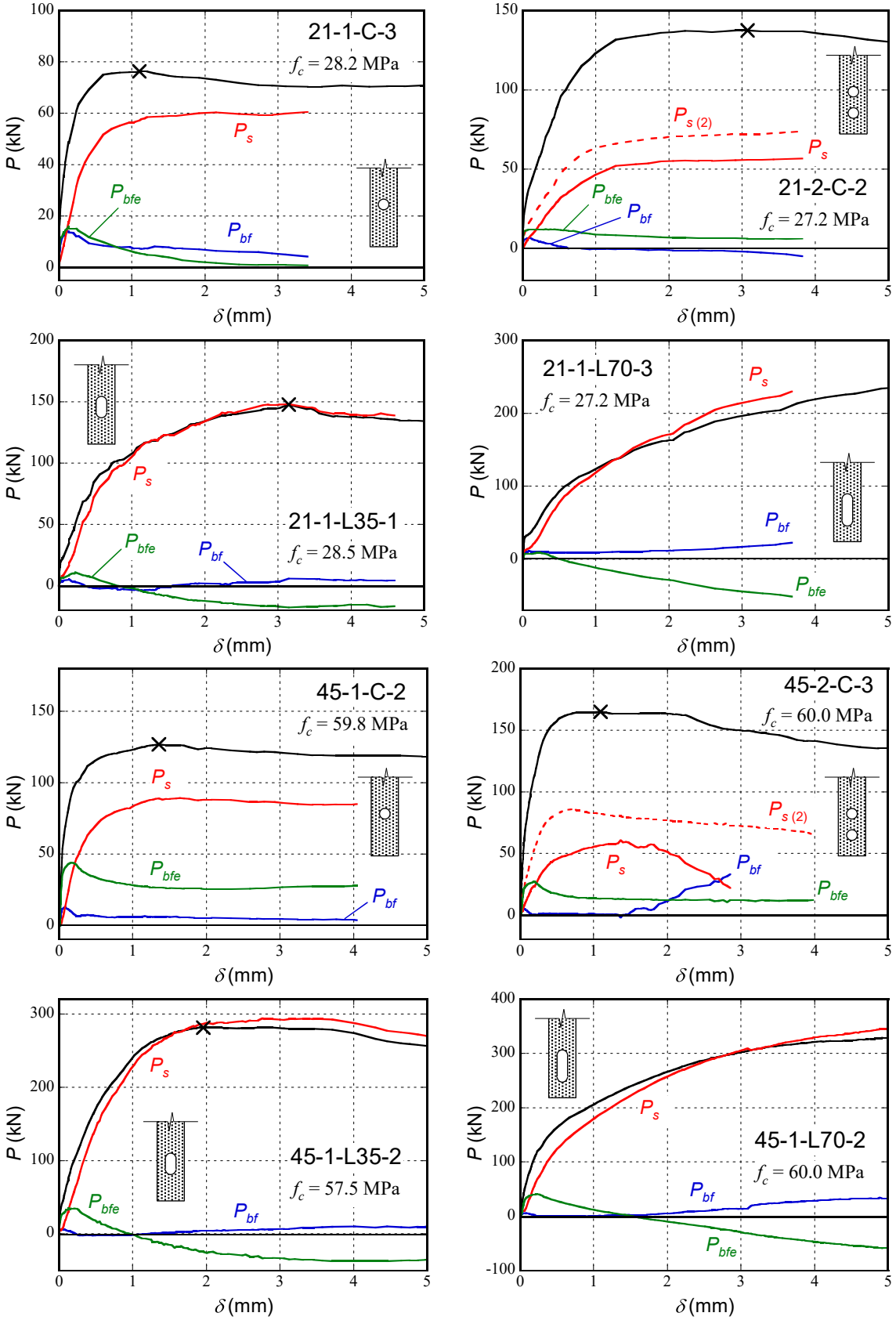

FIGURE 10. Bearing force versus relative slip displacement relationship

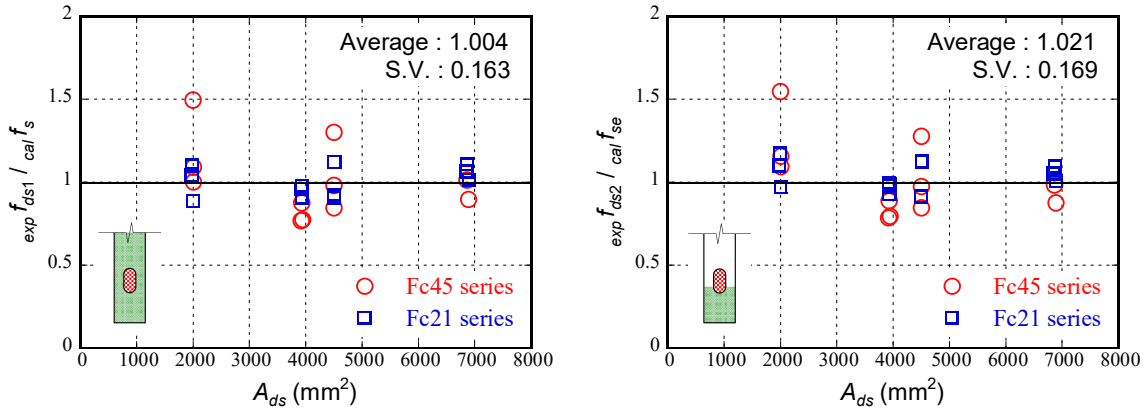

FIGURE 11. Relationship between the shear stresses at the perforation and shear area

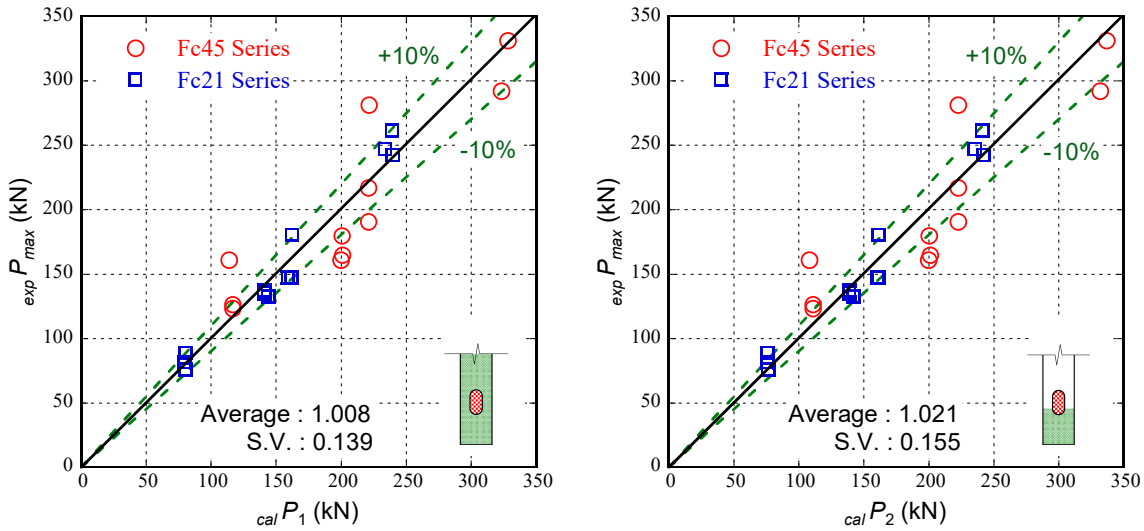

FIGURE 12. Comparison of experimentally obtained maximum and predicted pull-out strengths

resistance was calculated by applying the following procedures:

1 The axial force in a certain section was derived by multiplying the Young's modulus times the average strain of a certain section with strain gauges.
2 The shear resistance at the perforation (P_s) was determined as the difference between the axial forces above and below the perforation.
3 The bond and /or friction resistance (P_{bf}, P_{bfe}) was determined using axial forces above the first perforation and below the deepest perforation.

Figure 10 provides an example of the relationship between the bearing force and relative slip displacement. The black lines indicate the pull-out force and relative pull-out displacement relationship shown in Figure 7, and the red, blue, and green lines correspond to the shear resistance at perforation (P_s), bond and/or friction resistance above the first perforation (P_{bf}), and bond and /or friction resistance below the deepest perforation (P_{bfe}), respectively. The cross marks indicate the maximum pull-out strength.

The bond and/or friction resistance above the first perforation with respect to the entire pull-out force was very small compared with the other resistance values, regardless of the perforation shape. The relative slip displacement at the maximum bearing bond and/or friction resistance was <0.5 mm, which is considerably small. The bearing ratio of the bond resistance was large at a small relative slip displacement; however, that of the double shear resistance increased with the slip displacement. The largest contributor to the bearing ratio in the pull-out force was the double shear of concrete at the maximum pull-out strength. The bond and/or friction resistance above the perforation was almost zero at the maximum pull-out strength. Further, the bearing pressure from the concrete in the perforation was included below the perforation in the bond and/or friction resistance as a negative strength; therefore, the actual bond and/or friction resistance could not be appropriately evaluated after an increase in the bearing shear force at the perforation.

3. Strength Evaluation of Perforated Steel Plates

The effect of concrete strength on shear stress $_{cal}f_s$ was evaluated in the bond and/or friction area of the perforated steel

TABLE 3. Comparison of experimentally obtained and calculated strengths

Specimens	${}_{exp}P_{ds}$ (kN)	${}_{cal}P_{ds}$ (kN)	${}_{exp}P_{ds}/{}_{cal}P_{ds}$	${}_{cal}P_{u}$ (kN)	${}_{exp}P_{max}/{}_{cal}P_{u}$
21-1C-1	71.5	64.9	1.101	80.2	1.113
21-1C-2	67.6	64.6	1.046	79.9	1.023
21-1C-3	57.9	65.3	0.887	80.6	0.946
21-2C-1	117.2	129.0	0.908	143.8	0.923
21-2C-2	123.7	126.7	0.977	140.9	0.976
21-2C-3	121.4	126.4	0.961	140.7	0.961
21-1L35-1	133.7	147.5	0.907	162.1	0.910
21-1L35-2	166.3	147.9	1.124	162.4	1.111
21-1L35-3	133.9	144.9	0.924	159.0	0.926
21-1L70-1	229.9	226.2	1.016	239.9	1.010
21-1L70-2	249.4	225.4	1.107	239.0	1.095
21-1L70-3	234.6	220.7	1.063	233.9	1.056
45-1C-1	89.0	88.6	1.005	116.5	1.060
45-1C-2	96.5	88.3	1.092	116.5	1.088
45-1C-3	129.5	86.5	1.497	113.8	1.415
45-2C-1	133.2	173.1	0.769	199.8	0.806
45-2C-2	152.2	173.3	0.878	200.3	0.898
45-2C-3	134.9	174.2	0.775	201.0	0.821
45-1L35-1	191.9	195.6	0.981	221.1	0.983
45-1L35-2	254.9	195.6	1.303	221.1	1.273
45-1L35-3	165.3	195.3	0.847	220.8	0.864
45-1L70-1	269.1	299.2	0.899	323.2	0.905
45-1L70-2	307.6	303.1	1.015	327.9	1.011

plates at the pull-out strength using the double shear strength at the perforation P_{ds}, which is considered the entire surface area of the steel plate on the long side of section A_b. The double shear strength of concrete at the perforation was expressed in an exponentiation form in this study for considering the effect of concrete strength. The exponent of the compressive strength of concrete, that is, the strength ratio with the double shear strength at the measured maximum pull-out strength P_{ds}, which has an almost linear relationship regardless of the concrete strength, was approximately 0.4. The shear stress used to predict the double shear stress at the maximum pull-out strength can be expressed as shown in Equation (3).

In the investigation of the bearing force presented in the previous section, the bond and/or friction force ratio above the first perforation was almost eliminated at the maximum pull-out strength. Here, the shear stress at the pull-out strength ${}_{cal}f_{se}$ was obtained, and only the surface area of the steel plate below the deepest perforation was considered as the effective bond and friction area A_{be}. The exponent of the compressive strength of concrete at which the strength ratio with double shear stress at the maximum pull-out strength f_{se} has an almost linear relationship was approximately 0.44. The shear stress used to calculate the double shear strength at the maximum pull-out strength can be expressed as shown in Equation (4).

$$ {}_{cal}f_s = 8.6 \times {f_c}^{0.4} \tag{3} $$

$$ {}_{cal}f_{se} = 7.8 \times {f_c}^{0.44} \tag{4} $$

where ${}_{cal}f_s$ represents the double shear stress at the maximum pull-out strength. ${}_{cal}f_{se}$ represents the double shear stress at the maximum pull-out strength using the effective bond and friction area.

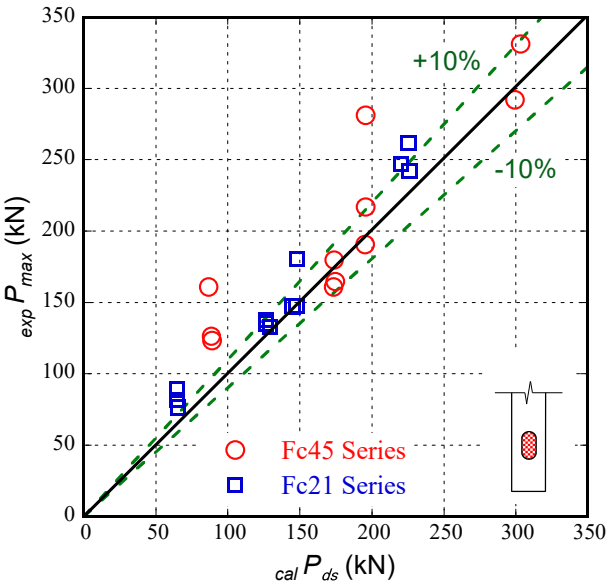

FIGURE 13. Comparison of experimentally obtained maximum and predicted double shear strengths

Figure 11 presents the relationship between the ratio of the shear stresses predicted using the shear stress given in Equations (3) and (4) and the measured double shear strength (see Section 2.3) and double shear area.

If it is assumed that the double shear strength at the perforation can be obtained by applying Equations (3) and (4) and the average bond and/or friction stress at the relative displacement of 2 mm $f_{bf,\ 2\,mm}$ can be used as the residual bond and/or friction stress at the maximum pull-out strength, the maximum pull-out strength of the perforated steel plates can be expressed as

$$_{cal}P_1 = {}_{cal}P_{ds} + f_{bf,2\ mm} \times A_b = {}_{cal}f_s \times A_{ds} + f_{bf,2\ mm} \times A_b \quad (5)$$

$$_{cal}P_2 = {}_{cal}P_{dse} + f_{bf,2\ mm} \times A_{be} = {}_{cal}f_{se} \times A_{ds} + f_{bf,2\ mm} \times A_{be} \quad (6)$$

where $_{cal}P_{ds}$ represents the double shear strength at the perforation, and $_{cal}P_{dse}$ represents the double shear strength at the perforation using the effective bond and/or friction area. Further, A_{ds}, A_b, and A_{be} represent the double shear area at the perforation, bond and friction area of the surface of the steel plate (entire surface area on the long side of the section), and effective bond and friction area of the steel plate surface (surface area below the center of the bottom arc of the perforation on the long side of the section), respectively.

Figure 12 compares the maximum pull-out strength and predicted pull-out strength, and Table 3 lists the experimental data and calculated strengths. As shown in Figure 12, Equations (5) and (6) can be used to estimate the experimental value regardless of the effective double shear area within about 10%. If the strength is determined by utilizing the double shear strength without using the residual bond and/or friction stress, the measured maximum pull-out strength can be estimated safely (see Figure 13).

4. Concluding Remarks

A pull-out experiment was conducted on a perforated steel plate with an oval-shaped perforation embedded in a CFST block. The following conclusions were drawn from the experimental results obtained for the 29 specimens used in this study.

1 The effect of concrete strength on both the maximum strength and the strength at a relative displacement of 2 mm was evaluated for specimens without perforations. The higher the concrete strength, the higher the measured strength.
2 A linear relationship was observed between the double shear strength at the maximum pull-out strength and the double shear area of the concrete in the perforation for the perforated steel plate specimens. The effect of the concrete strength was evaluated, and it was observed that the higher the concrete strength, the higher the maximum strength.
3 The larger the double shear area, the larger the relative slip displacement at a strength 0.9 times the maximum pull-out strength. The relative slip displacement at the maximum strength decreased at a higher concrete strength.
4 The largest contributor to the bearing ratio in the pull-out strength was the double shear of concrete in the perforation at the maximum strength. The bond and/or friction resistance above the perforation was very small.
5 Two types of effective bond and/or slip areas were examined, and formulas for the maximum pull-out strength were developed. The predicted strength can be used to estimate the measured maximum strength effectively within about 10%. If the strength is determined by using only the double shear strength, the maximum pull-out strength can be estimated safely.

The formulas developed in this study are valid only for the range of experimental parameters considered. However, a more appropriate coefficient for the formulas can be determined if perforated steel plate experiments are conducted using more comprehensive parameter ranges. Developing an appropriate design formula for the perforated steel plates and establishing a design method for the CFST column splices are subjects for future studies.

Acknowledgments

This research was funded by the Japan Society for the Promotion of Science, Grant-in-Aid for Scientific Research (C) (Grant number 20K04771), and by the Japan Iron and Steel Federation. The authors are grateful to Ms. Yuka Nagaoka and Mr. Kenta Tsuchiya for their helpful discussions.

Disclosures

The author has no conflict of interest to declare.

Data Availability Statement

The data that support the findings of this study are available from the corresponding author upon reasonable request.

References

1 Architectural Institute of Japan. *Recommendations for Design and Construction of Concrete Filled Steel Tubular Structures*. 2nd ed.; 2008. (in Japanese).
2 Sadamoto N, Fujinaga T. Experimental study on CFT column splice using perfobond rib shear connectors. *Summaries of Technical Papers of Annual Meeting. AIJ*. 2017:1429-1430. (in Japanese).
3 Leonhardt F, Andra W, Andra HP, Harre W. Neues, vorteilhaftes Verbundmittel fur Stahlverbund—Tranwerke mit Hoher Dauerfestigkeit. *Beton- und Stahlbetonbau*. 1987:325-331. (in German).
4 Architectural Institute of Japan. *Recommendations for Structural Design of Steel-concrete Shear Connections*; 2022. (in Japanese).
5 Nagaoka Y, Fujinaga T, Tanaka T. Influence of bond and friction on tensile strength of perforated steel plate connector under confinement. *Proceedings of International Structural Engineering and Construction*; 2021.
6 Zheng S, Liu Y, Yoda T, Lin W. Parametric study on shear capacity of circular-hole and long-hole perfobond shear connector. *J Constr Steel Res*. 2016;**117**:64-80.
7 Ido S, Tanaka T, Sakai J. Development of new mechanical shear connector using burring steel plate Part.9 push-out test for narrow section installation type. *Summaries of Technical Papers of Annual Meeting. AIJ*. 2020:1325-1326. (in Japanese).
8 Fukumoto T, Sawamoto Y. Friction and bonding behavior between steel and concrete under restriction stress. *J Struct Constr Eng Trans AIJ*. 2017;**82** (736):941-948. (in Japanese).

How to cite this article: Fujinaga T, Tanaka T. Pull-out strength of perforated steel plates with oval-shaped perforation. *Jpn Archit Rev*. 2023;6:e12363. https://doi.org/10.1002/2475-8876.12363